Enhancing the uncertainty quantification of pyroclastic density current dynamics in the Campi Flegrei caldera

Andrea Bevilacqua(1), Mattia de Michieli Vitturi(1), Tomaso Esposti Ongaro(1), Augusto Neri(1)

(1) Istituto Nazionale di Geofisica e Vulcanologia, Sezione di Pisa, Pisa, Italy.

ISTITUTO NAZIONALE DI GEOFISICA E VULCANOLOGIA

FISR-2017

Various aspect of the methodology are further described in: Bevilacqua et al. (2019), Probabilistic forecasting of plausible debris flows from Nevado de Colima (México) using data from the Atenquique debris flow, 1955. https://doi.org/10.5194/nhess-19-791-2019

1. Prediction-oriented modeling

In this study we present a new effort to improve the uncertainty quantification (UQ) of pyroclastic density current dynamics in the Campi Flegrei caldera, thanks to the implementation of a new 2D depth-averaged granular flow model in the Monte Carlo simulation of key-controlling variables. In this work, we set up a **plausible region** approach to provide a **prediction-oriented** probabilistic framework for hazard analysis (see also Bevilacqua et al. 2019 – this congress).

METHOD STEPS

(1) For a model M we define a probability measure P_M over the measurable parts of its feasible inputs Ω_0.

(2) We represent the model M with an operator: $f_M : \Omega_0 \longrightarrow \mathbb{R}^d$.

(3) Then, we characterize various examples of the codomain $D_G \subset \mathbb{R}^d$ of plausible outputs. They include the outputs consistent with potentially observed data, or verifying required constraints (see Fig. 1).

(4) We provide some examples of specialized input spaces defined by: $\Omega = f_M^{-1}[D_G \cap f_M(\Omega_0)]$. See Figure 1.

The implementation of **multiple models** is a desired aspect in this approach. Typically, a single model might not able to **entirely cover** D_G.

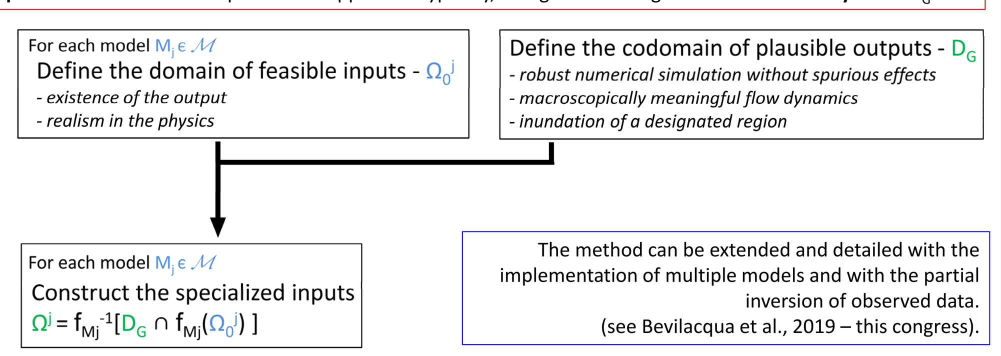

Fig 1. Diagram of the steps of our meta-modeling approach.

2. Geophysical case study

Campi Flegrei caldera is an active and densely populated volcanic area in the urban neighborhood of Napoli, characterized by the presence of many dispersed cones and craters, and by a caldera wall more than one hundred meters high, towards East. Pyroclastic density currents (PDC) are laterally moving, buoyantly expanding mixtures of hot gas and fragmental particles.

Basic mapping of PDC hazard at Campi Flegrei has been already reported in previous studies: some related to field reconstruction and numerical modeling of specific past eruptions or individual scenarios, while others endeavored to produce specific or integrated PDC hazard maps in which the variability of important parameters of the volcanic system was explicitly accounted for.

Figure 2. Example of temporal PDC invasion hazard map based on Bevilacqua et al., (2017), assuming that the volcano entered a new eruptive epoch in A.D. 1538. Contours and colors indicate the mean percentage probability of PDC invasion in the next 10 years.

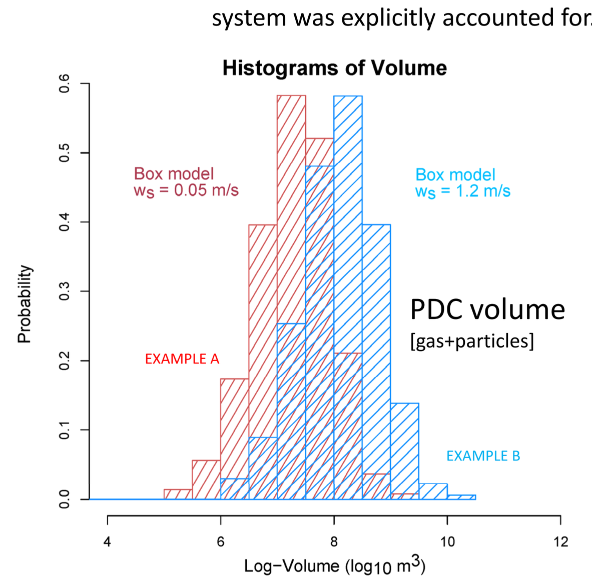

Figure 3. Results of Monte Carlo simulation varying the vent opening location (x, y) and the value of inundated area A, according to the probability models in Bevilacqua et al., (2017), with initial solid fraction of 1% volume.

In particular, Neri et al., (2015), Bevilacqua et al. (2017) obtained quantitative estimates of probabilistic PDC hazard, based on the implementation of a simplified kinematic invasion model able to represent main topographic effects (see Fig. 2).

This model is called **box model** because a cylindrical box represents the current and changes in aspect ratio (i.e. stretches out) as the flow progresses.

The statistical inversion of box model equations, varying the vent location (X, Y) and the value of inundated area A, provides us with initial probability estimates for the volume scale of the PDC flow, in terms of the volume extent of the multiphase mixture (see Fig. 3).

EXAMPLE A assumes a particle diameter of about 25 μm, and solid density 2000 kg/m³.

EXAMPLE B assumes a particle diameter of about 500 μm and solid density 1000 kg/m³.

Our depth averaged model relies on EXAMPLE B for setting up the volume scale of past flows.

3. Geophysical models and input spaces

We build our effort upon the previous research started in Todesco et al., (2006), Esposti Ongaro et al., (2016), and utilize the physical modeling approach of De Michieli Vitturi et al., (2019), with the efficient numerical solution of depth-averaged equations for the flow mass and momentum, considering the effects of basal and internal, velocity dependent, friction forces. We preliminarily adopt the **Voellmy-Salm** rheology (VS) (Voellmy, 1955; Salm, 1990).

UQ is performed by assuming three different components in the input space:
(i) source location, (ii) volume scale, (iii) rheology parameters.
Thus, the rheology and volume components of the input space are conjointly explored, attempting a hierarchical conditioning on feasible inputs and plausible outputs.

Further analyses with a second rheology describing the gas-particle mixture as a homogeneous flow, and assuming a mechanism of particle deposition consistent with that previously implemented in the box model, are currently in preparation.

The input spaces are explored by **Latin Hypercube sampling** (McKay, 1979; Stein, 1987). The model is parameterized by: $\Omega^{VS}{}_0 = (X, Y, \arctan(\mu), \log_{10}(\xi), V)$, contained in $\mathbb{R}^5$.

A first statistical analysis focuses on last three components, considering a fixed source location or an uncertain source location inside a subregion of the caldera. Afterwards, we show preliminary results also exploring the full spatial variability of the source location.

We enhance the sampling procedure by relying on orthogonal arrays (Owen, 1992; Tang, 1993)

Figure 4 displays the plot of our feasible input space. The spatial modeling of **random source locations** presents a new challenge compared to the study in Bevilacqua et al., (2019).

Uniform LHS are nonlinearly transformed according to the pdf of the input variables.

We study the effect of simple examples of conditioning, related to different **plausible outputs**, e.g. arbitrary minumum and/or maximum height at a specific site at the ending time.

This methodology can be focused on observed data, providing a partial inversion input space related to specific past PDC (see Bevilacqua et al. 2019)

We sample the input values in a **Monte Carlo** simulation. The output of each sample run is a function f(ω, x, t), where ω is the input, t is the time and x is a spatial element of the computational grid.
f is a **random function** with respect to the probability distribution P_M over Ω.

Feasible input domain $\Omega^{VS}{}_0$

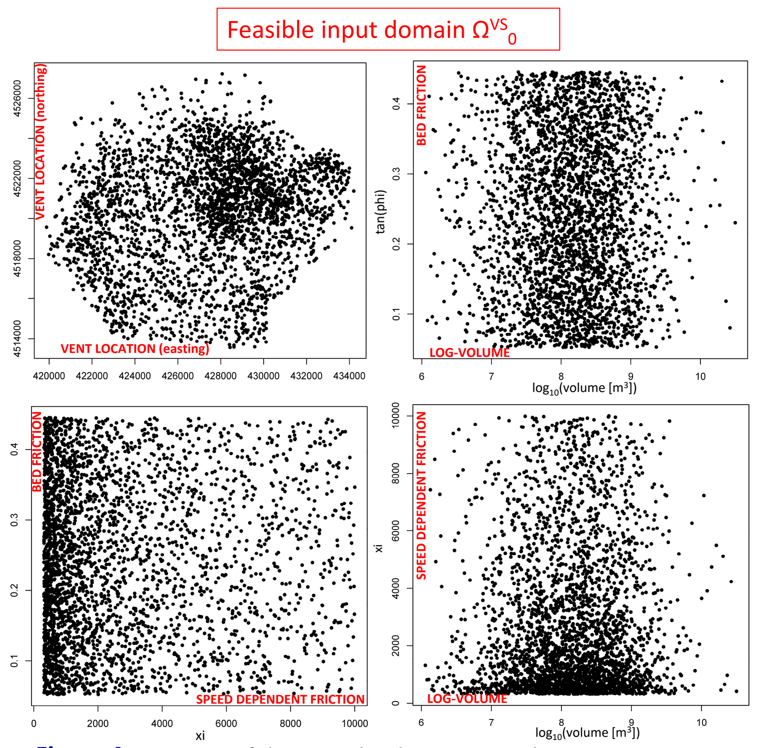

Figure 4. Overview of the specialized experimental.
2D projections along different coordinate pairs, reported on the axes.

4. Simulations with fixed vent location

Figure 5. Latin hypercube sampling based on orthogonal arrays of dimension 3.

The bed friction, the log-volume, and log(xi) are sampled uniformly over the following ranges:
φ in [3°, 24°]
$\log_{10}(\xi)$ in [2.5, 4]
$\log_{10}(V)$ in [6.95, 9.15]

The volume range is defined by the 5th and 95th percentiles of Example B.

In this simplified example the distribution of V differs from what shown in Fig.4, and does not follow the entire pdf of EXAMPLE B.

Feasible input domain

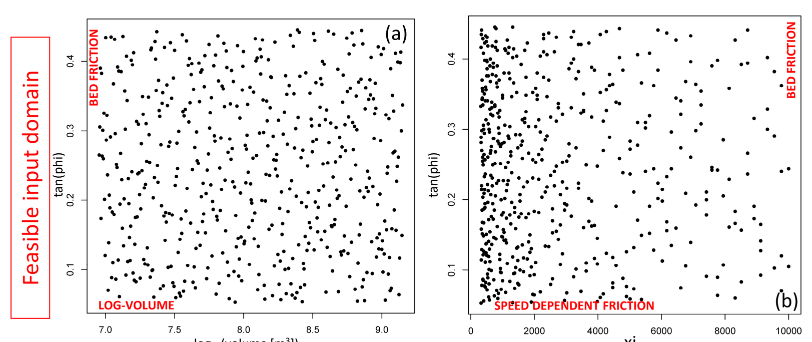

In this initial assessment the vent location is fixed at the arbitrary site: E 429000, N 4523000.

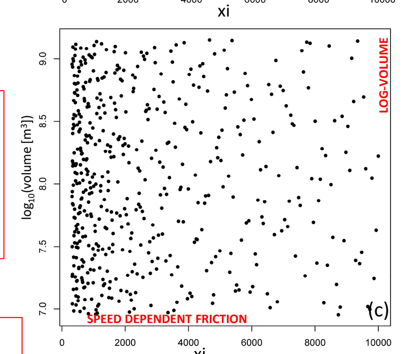

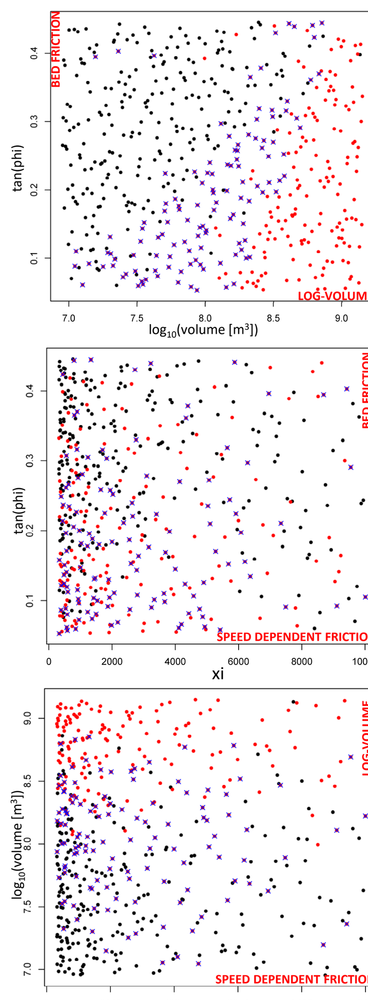

Specialized input domain $\Omega^{VS}{}_0$

Figure 6. Specialized input values which produce flows capable of invading a target location.

Red dots reach the arbitrary target site: E 430000 N 4521000

Blue crosses mark those inputs which leave < 20 m deposit at the target site after inundating it.

Over on the feasible input space we show:
- percentile maps of the flow height at the ending time;
- percentile maps of the max. simulated flow height;

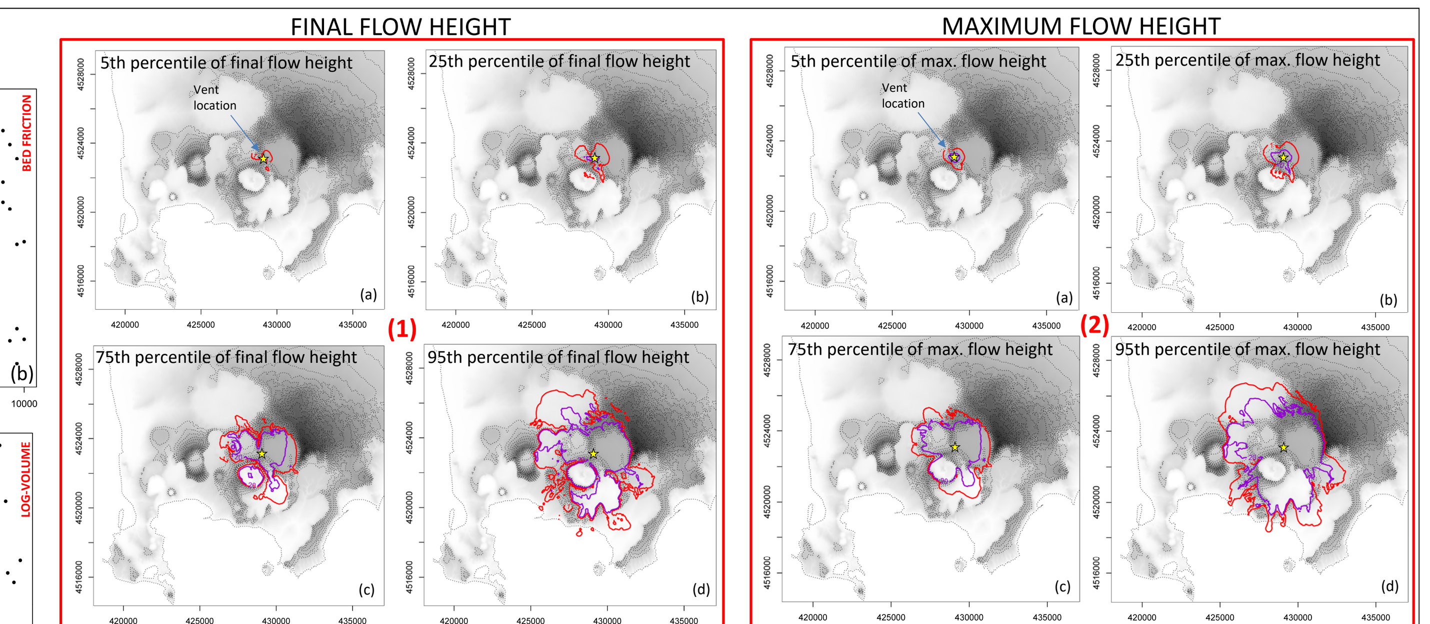

Figure 7. (1) Flow height statistics at the ending time t = 300 s, and ; (2) Maximum flow height statistics in the time interval t in [0 s, 300 s]. Flow dynamics is typically concluded in 60 - 90 s. Vent location is not varied, it is fixed at the arbitrary site: E 429000 N 4523000.

Red contours are 1 m flow height, purple contours are 20 m flow height. (a), (b), (c), (d) show the 5th, 25th, 75th, and 95th values respectively.

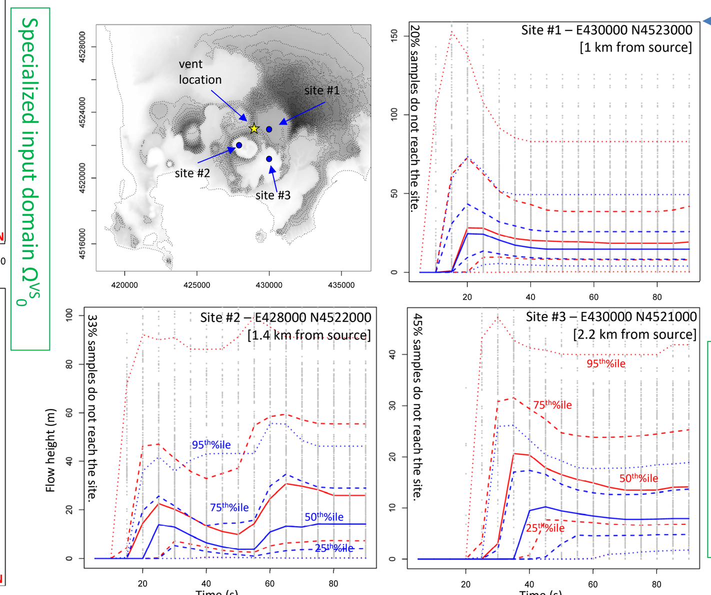

Figure 8. Flow height recorded at four arbitrary target sites.

5th, 25th, 50th, and 95th percentiles values are displayed as a function of time, with a time step of 5 s.

The statistics are conditional on reaching the sites. Red lines are unconditional, blue lines are conditional on invading site #4.

Based on the specialized input space we show conditional maps:
- probability of exceeding a 1 m flow height threshold at the ending time
- probability of exceeding a 1 m flow height threshold as the maximum value.

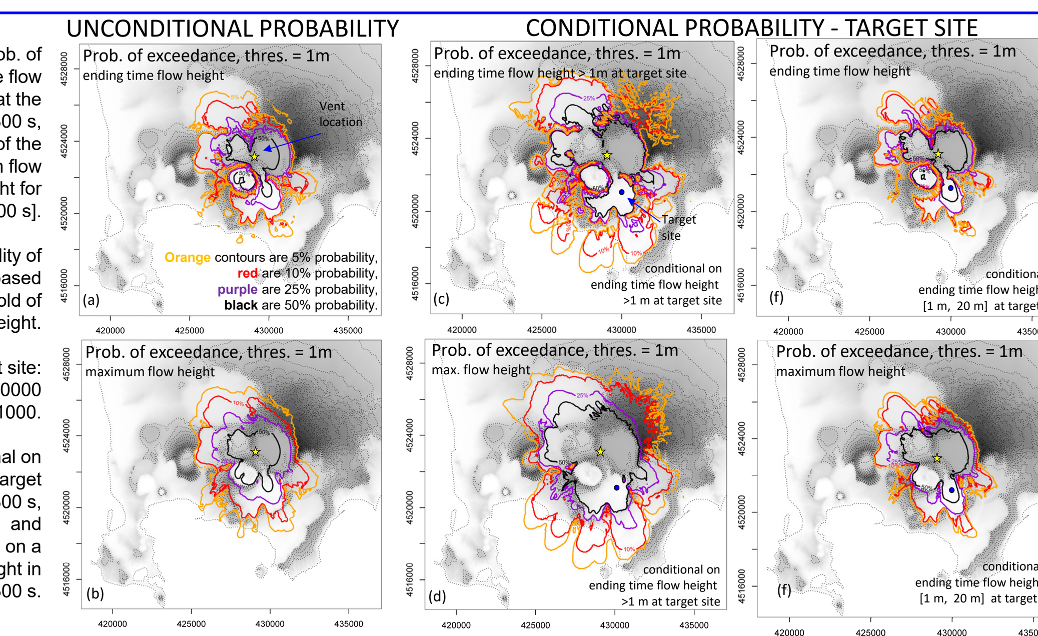

Figure9. Prob. of exceedance of the flow height (a,c,e) at the ending time t = 300 s, and (b,d,f) of the maximum flow height for t in [0 s, 300 s].

The probability of exceedance is based on a threshold of 1 m flow height.

Arbitrary target site: E 430000 N 4521000.

(c,d) conditional on inundating the target site, >1 m at 300 s, and (e,f,) conditional on a flow height in [1 m, 20 m] at 300 s.

5. Simulations with locally varying vent location inside subregions

Figure 10. Latin hypercube samples classified with respect to the caldera zonation of Bevilacqua et al., (2015). The numbers display the counting of the samples belonging to each zone.

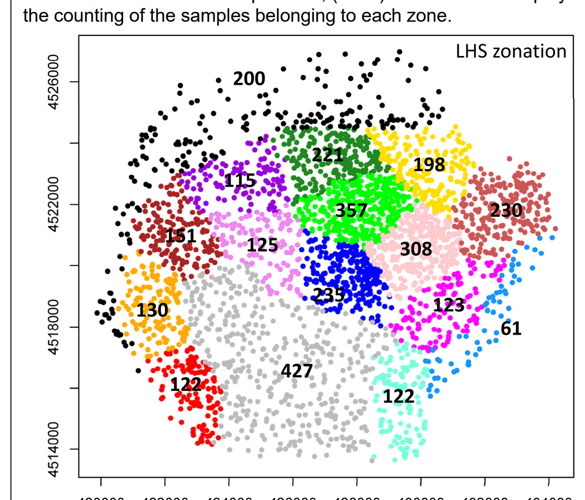

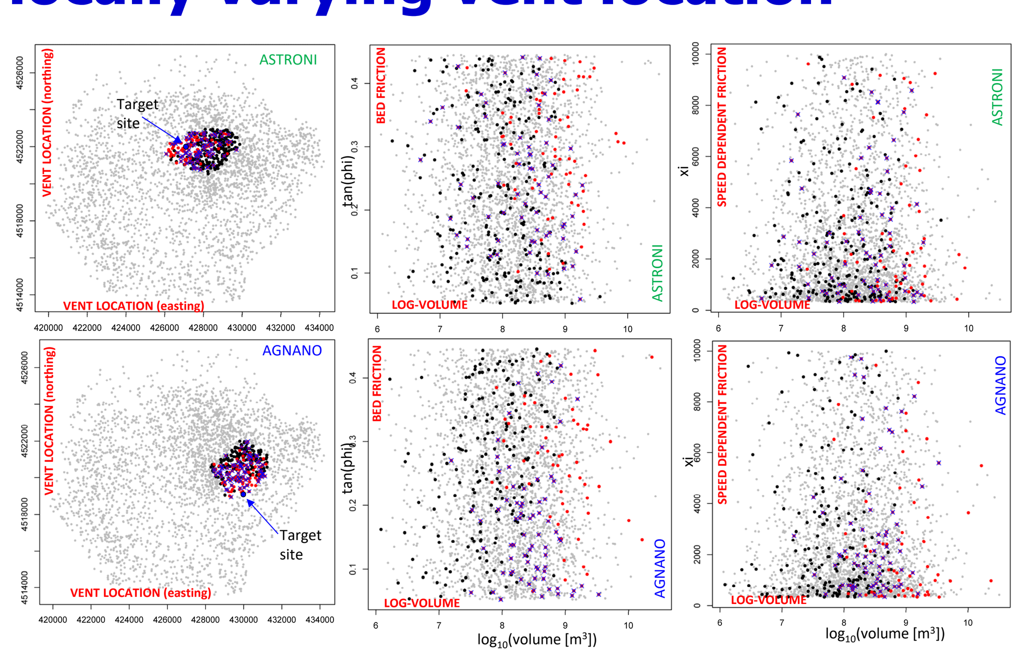

Figure 11. Specialized input values which produce flows capable of invading an arbitrary target location. Vent location is varied inside Astroni zone (357 values), Agnano zone (308 values). The grey dots are not considered because outside the zone. Red dots reach the target site.
Blue crosses mark those inputs which leave < 20 m deposit at the target site after inundating it.

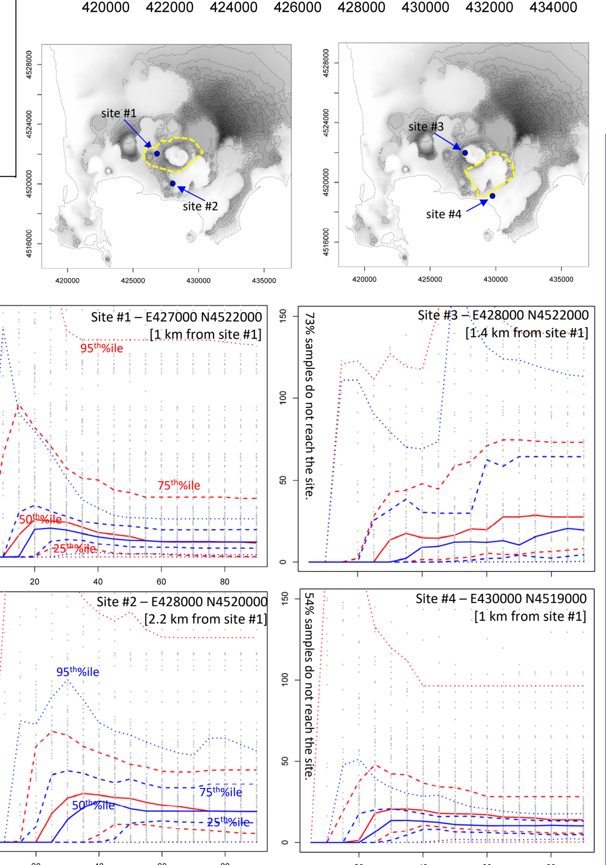

Figure 12. Flow height recorded at four arbitrary target sites. Vent location is varied inside Astroni zone (357 values), Agnano zone (308 values).

25th, 50th, and 95th percentiles values are displayed as a function of time, with a time step of 5 s. The statistics are conditional on reaching the sites. Red lines are unconditional, blue lines are conditional on invading the target site.

5th percentiles are included, but are negligible.

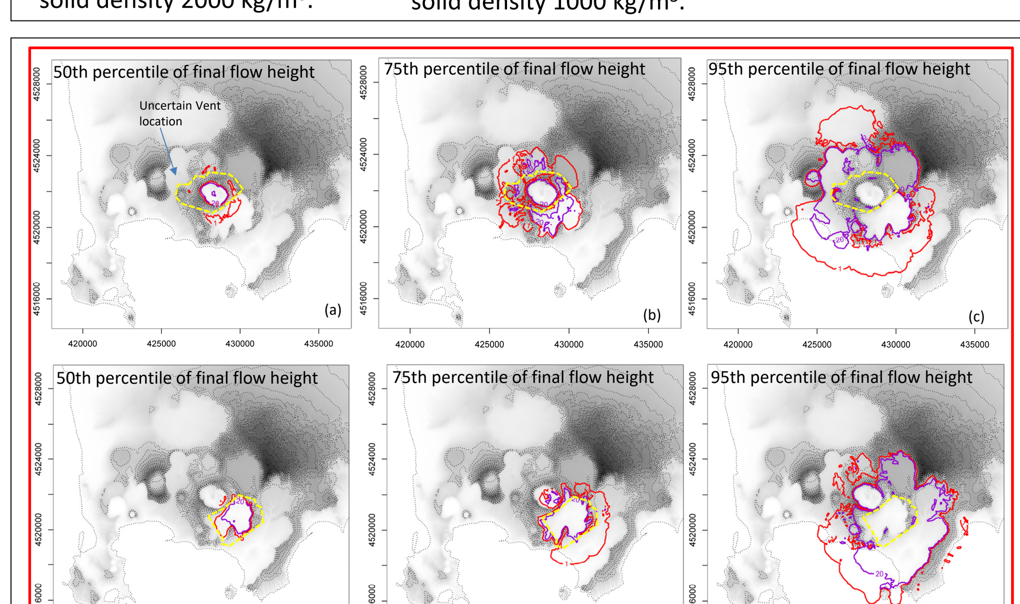

Figure 13. Flow height statistics at the ending time t = 300 s. Flow dynamics is typically concluded in 60 - 90 s.
Vent location is varied inside Astroni zone (357 values), Agnano zone (308 values).
Red contours are 1 m flow height, purple contours are 20 m flow height.
(a,d), (b,e), (c,f) show the 50th, 75th, and 95th values respectively.

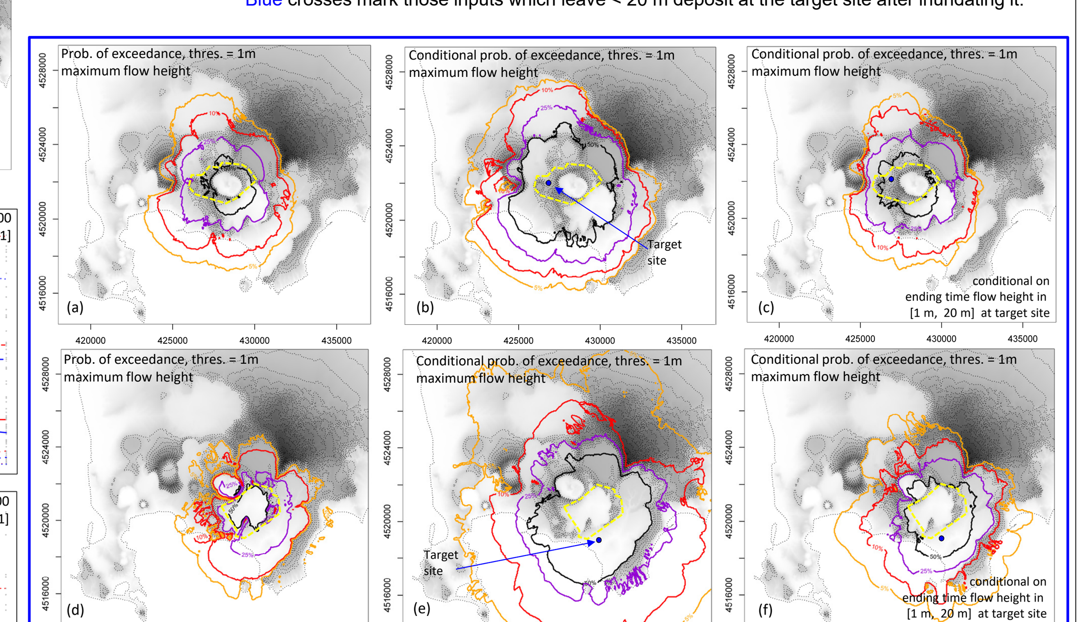

Orange contours are 5% probability, red are 10%, purple are 25% probability, black are 50%.

Figure 14. Probability of exceedance of the maximum flow height for t in [0 s, 300 s].
Vent location is varied inside Agnano zone (308 values), Astroni zone (357 values).
The probability of exceedance is based on a threshold of 1 m flow height.
In (b,e) the flow is conditional on invading the target site: E 427000 N 4522000 in the Astroni example, E 430000 N 4519000 in the Agnano example.
(e,f) are conditional on a flow height in [1 m, 20 m] in the target site at 300 s.

6. Simulations with globally varying vent location

Specialized input domain $\Omega^{VS}{}_0$

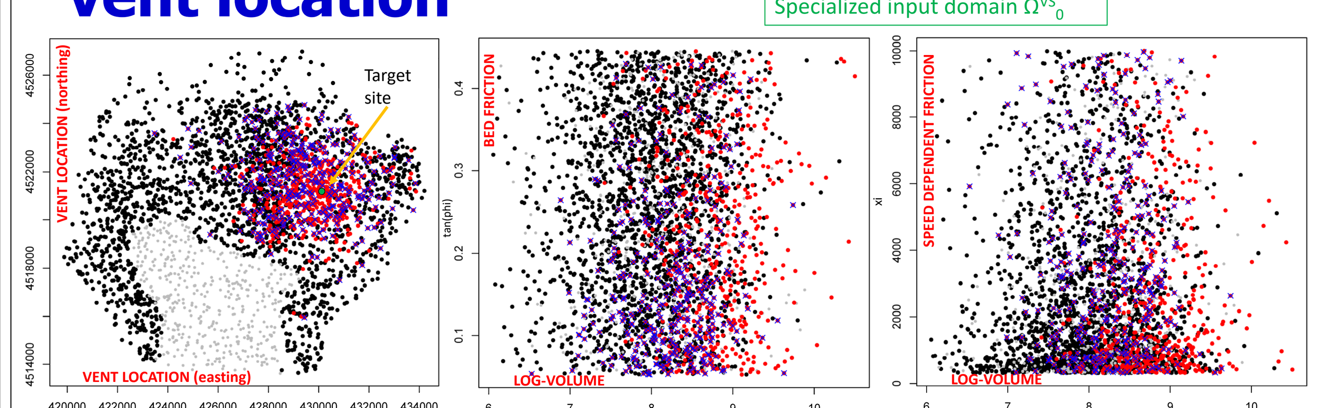

Figure 15. Specialized input values which produce flows capable of invading a target location. Vent location is varied over the entire region onland.
Red dots reach the target site: E 430000, N 4521000. Blue crosses mark those inputs which leave < 20 m deposit at the target site after inundating it.
Grey dots are those located underwater and not considered.

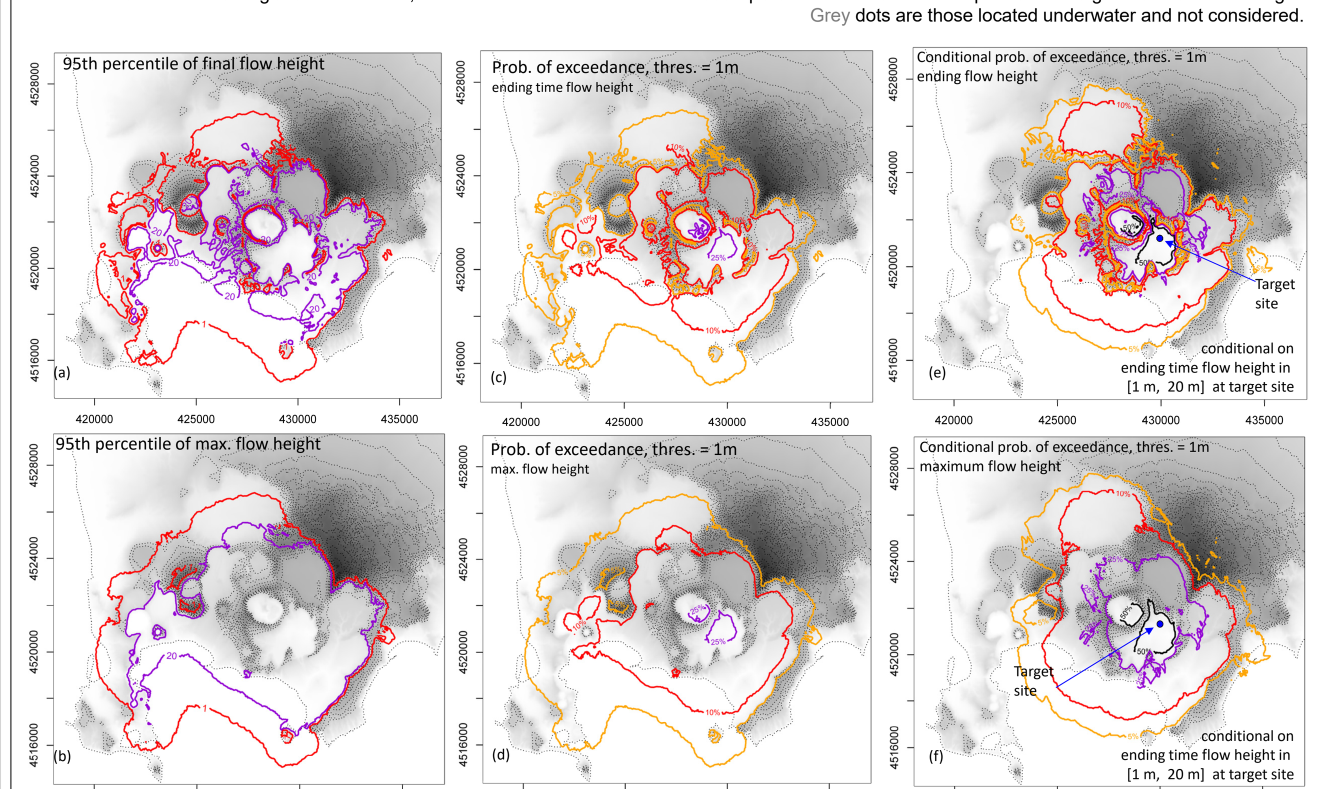

Orange contours are 5% probability, red are 10%, purple are 25% probability, black are 50%.

Figure 16. (a,b) 95th percentile values and (d-f) prob. of exceedance of the flow height (a,c,e) at the ending time t = 300 s, and (b,d,f) of the maximum flow height for t in [0 s, 300 s]. The prob. of exceedance is based on a threshold of 1 m flow height. Arbitrary target site: E 430000, N 4521000. (e,f) are conditional on a flow height in [1 m, 20 m] in the target site at 300 s.

Acknowledgements: This work is supported by Italian Ministry of Education, University, and Research, project FISR2017 – SOIR, and by National Science Foundation award 1821311.

7. Conclusions

We introduced a new prediction-oriented method for hazard assessment of PDC and tested its application to Campi Flegrei caldera (Italy).

In summary:

- We defined a five dimensional feasible input space describing the spatial location (x,y) of the PDC source, the volume V of the flow, and the rheology parameters (φ, ξ in Voellmy-Salm model).
- The probability distribution over the input space was based on the results of the previous research in Bevilacqua et al., (2015), Neri et al., (2015) and Bevilacqua et al., (2017), also relying on the statistical inversion of a simplified model. The Voellmy-Salm rheology parameters were distributed uniformly over their range.
- We run a SW numerical solver of De Michieli Vitturi et al., (2019) over the entire feasible input space, and statistically explored the outputs. First we focused on a fixed vent location, then on a locally varying vent, and finally we considered the globally varying general case.
- In particular, we produced percentile maps of the flow height at the ending time, percentile maps of the max. simulated flow height, probability maps of exceeding a 1 m flow height threshold, either at the ending time or as the maximum value. We also estimated the flow height percentiles as a function of time in specific locations.
- Then we described various specialized input spaces after assuming the condition of a flow height at the ending time greater than 1 m or included in [1m, 20 m].
We compared the effect of this conditioning on the ending flow height and the max. flow height.

Future research will be focused on:

- The development of a second model including a mechanism of particle deposition, which is believed to have been a very important process determining the PDC dynamics in this region. That indeed was the physics at the base on the box model idea.
- The partial inversion of the data available about specific past flows (some are well reconstructed in literature), rather than or in addition to an improved plausible conditioning.

References:

Bevilacqua, A. et al. (2015), Journal of Geophysical Research: Solid Earth, 120, 2309-3329.
Bevilacqua, A. et al. (2017), Frontiers in Earth Science, 5, 72.
Bevilacqua, A. et al. (2019) Natural Hazards Earth System Science, 19, 791-820.
De' Michieli Vitturi et al. (2019), Geoscientific Model Development, 12, 581-595.
Esposti Ongaro et al. (2016), Journal of Volcanology and Geothermal Research 327, 257 – 272.
McKay, M.D., Beckman, R. J., and Conover, W. J. (1979), Technometrics, 21, 239–245.
Neri, A. et al. (2015), Journal of Geophysical Research: Solid Earth, 120, 2330-2349.
Owen, A.B.(1992), Statistica Sinica, 2, 439–452.
Salm, B. (1993), Annals of Glaciology, 18, 221–226.
Stein, M. (1987), Technometrics, 29, 143–151.
Tang, B. (1993), Journal of the American Statistical Association, 88, 1392–1397.
Todesco, M. et al. (2006), Geochemistry Geophysics Geosystems, 7, Q11003.
Voellmy, A.(1955), Schweiz Bauzeitung, 73, 159–165, 212–217, 246–249, 280–285.